



Cite this: *Mater. Adv.*, 2022,  
3, 4991

## Biosynthesis of NiO nanoparticles using *Spirogyra* sp. cell-free extract and their potential biological applications

Yadvinder Singh,<sup>a</sup> Ramandeep Singh Sodhi,<sup>b</sup> Prit Pal Singh <sup>\*b</sup> and  
Sandeep Kaushal <sup>\*b</sup>

Biosynthesis is progressing owing to economical synthesis and the availability of organisms (good source of metabolites) which significantly complex and cap the metallic ions to produce stable nanomaterials. In this study, nickel oxide nanoparticles (NiO NPs) were prepared using cell free extract of *Spirogyra* sp., a filamentous green macroalgae containing polyols, amines, and carbonyl compounds. The biomolecules in the extract efficiently convert  $\text{Ni}(\text{NO}_3)_2$  to NiO as indicated by a change in color from greenish to reddish violet. The formation of NiO NPs was confirmed by the signature peak observed at 350 nm in the UV spectrum and diffraction peaks at  $2\theta = 37.3, 43.3, 62.9$  and  $75.6^\circ$  in the XRD spectra. The crystallite size of the as-synthesized NiO NPs was calculated to be 27.7 nm. The physical characterization techniques like FESEM, HRTEM etc. confirmed the formation of polycrystalline quasi-spherical NPs. The synthesized material was further investigated for its potency for biological applications. Its antibacterial action ( $\text{IC}_{50}$ : 10 mg L<sup>-1</sup>) against Gram-positive (*Bacillus subtilis*) and Gram-negative (*Escherichia coli*) bacterial strains showed concentration dependent activity with MIC (minimum inhibitory concentration) of 10 mg L<sup>-1</sup>. In addition, the NPs showed a stimulatory effect at lower concentration (5 mg L<sup>-1</sup>) with a nearly 15% increase in the root length and shoot length, while they exhibited an inhibitory effect at higher concentration ( $>5$  mg L<sup>-1</sup>) on seed germination and seedling growth of Mung Beans (*Vigna radiata* (L.) R. Wilczek). In addition, the NiO NPs showed appreciable antioxidant potential, evaluated through assays like DPPH and TAC. Furthermore, it is concluded that the as-synthesized NiO NPs via a green approach showed reliable *in vitro* biochemical properties, which signifies their potential for use in the biomedical and agricultural fields with future appraisal.

Received 2nd February 2022,  
Accepted 29th April 2022

DOI: 10.1039/d2ma00114d

rsc.li/materials-advances

## Introduction

Small particles with wider pertinence have revolutionized the field of nanotechnology. Sustainable growth in this field has been observed in the last decade as nanomaterials display distinct characteristics responsible for their diverse acceptability and utilization.<sup>1</sup> Global efforts have been made for large-scale production of nanomaterials, considering their advantageous physical, chemical, and biological properties. The conventional methods employed for their synthesis have restricted their applications in the field of ecological remediation, photocatalysis, biomedicine and agriculture.<sup>2,3</sup> The challenge in the

current situation is to develop efficient, rapid, reputable and biological approaches for the synthesis of stable nanomaterials for their widespread biological applicability. Looking at the abundant availability of flora and fauna, researchers have been probing continuously the suitable candidates for bio-synthesis of nanomaterials. The bottom down biogenic approach has gained prominence due to its affordable cost, less complexity and environment friendly nature.<sup>4–6</sup> Numerous organisms like plants, fungi, algae, bacteria etc. have been utilized by different workers for the synthesis of metal/metal oxide NPs.<sup>7–9</sup> The metabolic byproducts from organisms act as reducing, and capping agents to improve stability and biocompatibility.<sup>10,11</sup>

Algae, as one of the dominant photosynthetic and diverse primitive organisms, are a rich source of secondary metabolites, proteins, peptides, and pigments.<sup>1</sup> Algae also have high metal accumulation capacity and the ability to transform metals into NPs either intra or extra-cellularly. The members of various classes of algae such as Cyanophyceae (blue-green algae/cyanobacteria), Phaeophyceae (brown algae), Chlorophyceae

<sup>a</sup> Department of Botany and Environmental Science, Sri Guru Granth Sahib World University, Fatehgarh Sahib, Punjab, India

<sup>b</sup> Department of Chemistry, Sri Guru Granth Sahib World University, Fatehgarh Sahib, Punjab, India. E-mail: kaushalsandeep33@gmail.com, dhillonps2003@gmail.com; Fax: +91-1763-234236; Tel: +91-7009795652, +91-8427000415



(green algae), and Rhodophyceae (red algae) have been exploited for the synthesis of metallic and metal oxide NPs.<sup>1,12</sup> Although, Ag, Au and Zn NPs have been synthesized using algal extracts, *i.e.* ZnO using *Sargassum muticum*,<sup>9</sup> Ag NPs using *Bacillus brevis* and marine algae *Spirogyra* and *Padina sp.*,<sup>11,13</sup> and Au NPs using aqueous algal extract of *Laminaria japonica*,<sup>14</sup> there is still scope to explore the potential of more algal species for the synthesis of unique nanomaterials.

Commercially, among metallic NPs, nickel nanoparticles have attracted considerable interest owing to their intrinsic semiconductor properties, electron transfer capability, antimicrobial and anti-inflammatory potential and admirable magnetic and electrical properties.<sup>2–4</sup> In comparison to nickel nanomaterials synthesized chemically, the green approach produces nanomaterials having diminished size with excellent monodispersity, which demonstrate enhanced *in vitro* biological applications.<sup>15</sup> Currently, few reports are available on biogenic synthesis of Ni NPs by employing various plants and plant products. The bio-fabricated Ni and NiO nanoparticles using extracts from plant sources *Hordeum vulgare*, *Ananas comosus*, *Ocimum sanctum*, *Calotropis gigantea*, *Brassica rapa*, *Alfalfa* and *Stevia* leaf have shown reliable *in vitro* biochemical properties.<sup>2,15–19</sup> The reports signify the utility of biogenic Ni NPs in biomedical and agricultural fields due to their conducting nature, controlled size, ability to generate oxidative stress and inherent anti-pathogenic properties.<sup>4</sup> Khan *et al.* observed the stimulatory effect of doped Ni NPs on germination of wheat and pearl millet seeds, which might be due to the embedding of controlled size NPs through the seed coat, which activated the embryonic uptake of nutrients along with water.<sup>18</sup>

The current study describes an efficient biological method for the synthesis of NiO NPs using a cell-free extract of macroalgae *Spirogyra* sp. To the best of our knowledge, NiO NPs have been obtained for the first time using macroalgae *Spirogyra* sp. The NiO NPs were characterized by FTIR, XRD, FESEM, EDX, HRTEM, BET, XPS and RAMAN spectroscopic techniques to explore their potential for *in vitro* biochemical applications. The antibacterial potential was evaluated against one Gram negative (*Escherichia coli*) and one Gram positive (*Bacillus subtilis*) bacteria along with antioxidant properties in terms of DPPH and OH radical scavenging activity. Moreover, the effect of the synthesized NiO NPs on seed germination and early seedling growth of mung beans has been studied to evaluate its biocompatibility as well as multi-functionality for potential agricultural applications as a seed priming agent. The results revealed that algal metabolites have the potential to work as a complexing and stabilizing agent for the synthesis of NiO NPs. The synthesized environment friendly NiO NPs have potential for widespread future applications in medical and agricultural fields.

## Materials and methods

### Collection and identification of algal biomass

The biomass of filamentous green macroalgae was collected from a freshwater stream, near Rajpura city of Punjab, India.

The collected biomass was washed with double distilled water (DDW) several times to remove impurities. *Spirogyra* sp. was identified according to the following morphological characteristics: vegetative cells 85–230  $\mu\text{m}$  long and 40–60  $\mu\text{m}$  wide; 1–5 chloroplasts spirally arranged; ellipsoidal zygospores.

### Preparation of cell free extracts

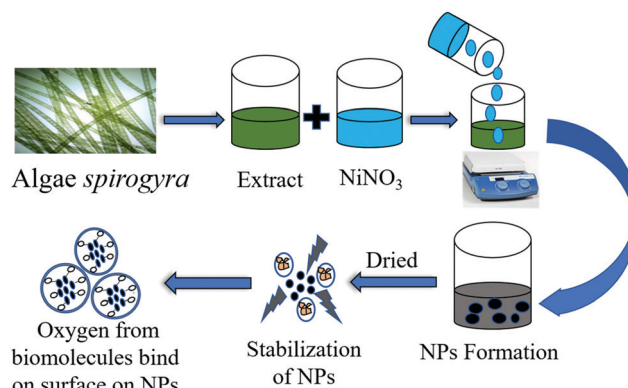
The cleaned biomass of *Spirogyra* sp. was dried in the shade at room temperature for a week and then pulverized using a pestle and mortar. To prepare the aqueous cell free extract, 10 g pulverized biomass was mixed with 100 mL DDW taken in a 250 mL conical flask, and the mixture was kept in a boiling water bath for 30 min with continuous stirring. Then, the mixture was centrifuged at 12 000 rpm for 10 min and the obtained greenish supernatant liquid (cell free extract) was stored at 4 °C in a refrigerator for further use.

### Synthesis of NiO NPs

The aqueous cell free extract (10 mL) obtained above was added dropwise into 100 mL of 0.05 M  $\text{Ni}(\text{NO}_3)_2$  (AR grade) solution taken in a 250 mL conical flask. The pH of the reaction mixture was adjusted between 5–10 using sodium hydroxide, and kept at 65 °C for 30 min with constant mechanical stirring. The change in color of the solution from greenish to brownish red indicated the formation of NiO NPs. The nanoparticle synthesis process was monitored by UV-vis spectrophotometer. The solution mixture was cooled to room temperature and centrifuged at 14 000 rpm for 15 min. The pellet of NPs obtained was retained while the supernatant was discarded.<sup>20</sup> The obtained semi gel pellet of NPs was dried in an oven by heating at 100 °C for 1 h, followed by calcination at 400 °C for 4 h. The probable mechanism for the synthesis of NiO NPs is given in Scheme 1.

### Characterization of the synthesized NiO NPs

The optical properties of the synthesized material were evaluated by UV-visible spectrophotometer (Shimadzu-1800). Functional group analysis was done with an FTIR spectrophotometer (Perkin Elmer spectrophotometer-RXI). An X-ray diffractometer (Rikaguminiflex 600) was used for XRD analysis using  $\text{Cu-}\alpha$  radiation ( $\lambda = 1.54 \text{ \AA}$ ) operated at 40 kV and 15 mA with a



Scheme 1 Schematic for the step-wise synthesis of NiO NPs.



scanning speed of  $4.000^{\circ} \text{ min}^{-1}$ . Morphology and elemental analysis were assessed by field-emission scanning electron microscope (ZEISS) and high resolution transmission electron microscope (HRTEM). The surface area, total pore volume and mean pore diameter were determined using a BET (Bel, Japan, Inc, Microtec BELSORP MINI-II) surface area analyzer. Raman spectroscopic analysis was carried out using a Horiba, Model: Lab RAM HR evolution. The elemental composition, empirical formula, chemical state and electronic state were determined by X-ray photoelectron spectroscopy (XPS) (Thermo Fischer Scientific Escalab Xi +).

## Biological applications

### Antibacterial activity

The growth of both Gram-positive (*Bacillus subtilis*) and Gram-negative (*Escherichia coli*) bacterial strains was examined in the absence and presence of the synthesized NiO NPs. The pure cultures of each test organism were sub-cultured separately in 10 mL LB medium (Hi Media) by placing the culture vessel in a BOD incubator overnight at  $37^{\circ}\text{C}$  and 150 rpm agitation. Then, both the test organisms were again sub-cultured into 50 mL LB medium supplemented with different concentrations ( $2.5 \text{ mg L}^{-1}$ ,  $5 \text{ mg L}^{-1}$ ,  $10 \text{ mg L}^{-1}$  and  $15 \text{ mg L}^{-1}$ ) of synthesized NiO NPs by adjusting the initial optical density (OD) of the bacterial culture to 0.1 at 600 nm using a UV-visible spectrophotometer. The bacterial growth in culture supplemented by NiO NPs was measured periodically (after intervals of 2 h) in terms of the optical densities at 600 nm in comparison to the control (growth medium without NiO NPs) and algal cell free extract supplemented bacterial cultures. The experiment was performed in completely randomized design with three replications to record the growth of test organisms for 16 h, and the measured optical densities were plotted as a function of time.

### Antioxidant activity

#### DPPH

The antioxidant activity of the synthesized NiO NPs was evaluated by the DPPH method (19). Various concentrations ( $5 \text{ mg L}^{-1}$ ,  $10 \text{ mg L}^{-1}$ ,  $20 \text{ mg L}^{-1}$  and  $40 \text{ mg L}^{-1}$ ) of NiO NPs were prepared in methanol to assess their free radical scavenging potential. To prepare the reaction mixture, a 1 mL solution of each concentration of NiO NPs was added to a freshly prepared DPPH (2,2-diphenyl-1-picrylhydrazyl) methanol solution ( $80 \mu\text{g mL}^{-1}$ ) and kept in the dark at room temperature for 30 min. The decrease in concentration of DPPH was monitored by measuring the absorbance of the reaction mixtures at 517 nm using a UV-vis spectrophotometer, with methanol as the reference blank cooled to room temperature. All samples were prepared in triplicate and their absorbance was recorded at 695 nm by a UV-vis spectrophotometer. All samples were run in triplicate and the DPPH radical scavenging ability of the NPs was expressed in % as follows:

$$\text{Inhibitions (I\%)} = \frac{\text{Absorbance of control} - \text{Absorbance of sample}}{\text{Absorbance of control}} \times 100$$

### Total antioxidant capacity

The total antioxidant capacity of the synthesized NiO NPs was determined using different concentrations of NPs ( $5 \text{ mg L}^{-1}$ ,  $10 \text{ mg L}^{-1}$ ,  $20 \text{ mg L}^{-1}$  and  $40 \text{ mg L}^{-1}$ ) by following the phosphomolybdenum method.<sup>21</sup> To prepare the reaction mixture, 400  $\mu\text{L}$  of the sample was mixed with 3.6 mL of reagent solution containing 0.6 M sulfuric acid, 28 mM sodium phosphate and 4 mM ammonium molybdate. The reaction mixture tubes were incubated at  $95^{\circ}\text{C}$  for 90 min and then the capacity of each sample was expressed as milligrams (mg) of ascorbic acid (AA) equivalent by taking ascorbic acid as a standard reference.

### Effect on seed germination and seedling growth

The effect of biogenically synthesized NiO NPs on seed germination and seedling growth was evaluated using Mung Bean (*Vigna radiata* (L.) R. Wilczek) seeds. To ensure the surface sterility, the seeds were sterilized with 5% sodium hypochlorite solution for 15 min and rinsed thoroughly with DDW several times. Different concentrations ( $5 \text{ mg L}^{-1}$ ,  $10 \text{ mg L}^{-1}$ ,  $20 \text{ mg L}^{-1}$  and  $40 \text{ mg L}^{-1}$ ) of the synthesized NPs were prepared for this experiment by mixing the powdered NiO NPs in sterilized DDW. The prepared aqueous nano-solutions were introduced in pre-sterilized Petri plates containing four layers of filter paper (Whatman filter paper) and 20 Mung Bean seeds. The cell free algal extract and DDW (without NiO NPs) were used as a control. A completely randomized design with three replications was employed and the experimental setup was kept in the dark at  $27^{\circ}\text{C}$ , to assess the phytotoxicity of the NiO NPs. The seed germination rate and the seedling growth in terms of root and shoot lengths were measured on the 4th and 8th day.

## Results and discussion

### Biosynthesis of NiO NPs

The cell free extract of *Spirogyra* sp. contains various biomolecules like tannin, phenolics, saponins, poly-alcohols, phenols, terpenoids, flavonoids, etc.<sup>22,23</sup> When nickel nitrate solution is incorporated in the aqueous algal extract, the nickel ions may interact with phytochemicals present in the aqueous *Spirogyra* sp. extract which form complexes with nickel ions, and a noticeable change of color is observed.<sup>24</sup> Various optimizations of the reaction conditions were explored prior to the synthetic process, and it was discovered that the volume of algal *Spirogyra* extract of 10 mL, pH 8 and the reaction duration of 30 min with constant stirring constituted the optimum conditions for synthesis. By using the above parameters, the NiO NPs were synthesized and the solutions were checked using a spectrophotometer for the formation of nanoparticles.<sup>25</sup> The synthesized particles were then washed with DDW and calcined to get NiO NPs in powder form.

### Physical characterization of the NiO NPs

Several analytical techniques were used to confirm the biosynthesis of NiO NPs. The change of color of the reaction



mixture from greenish to brownish red on mixing the precursor,  $(\text{NiNO}_3)_2$ , with algal cell free extract at  $65^\circ\text{C}$  indicated the formation of NiO NPs. The NPs synthesis was monitored using the UV-vis spectrophotometer absorption peaks positioned at 350 nm (Fig. 1a). The NPs suspension was preserved for 72 h at room temperature and surface plasmon resonance was studied after regular intervals using a spectrometer. The results showed a significant peak centered at 350 nm with diminished intensity, indicating the sedimentation of stable NiO NPs. The reports suggest the binding of biomolecules, protein or metabolites, *i.e.* amines, terpenoids *etc.*, which provide stability to the NPs.<sup>18</sup> The characteristic peaks of biomolecules have been observed in the IR spectra.

The signature peaks of different functional groups in the FTIR spectrum of *Spirogyra* sp. cell free extract (Fig. 1b) showed that many biomolecules present in the extract may act as capping and stabilizing agents during the process of synthesis.

The broad peak at  $3576\text{ cm}^{-1}$  is attributed to the O–H stretching mode of alcohols or polyols.<sup>11</sup> The weak bands at  $2928\text{ cm}^{-1}$  may be attributed to C–H stretching of hydrocarbons and the peak at  $2316\text{ cm}^{-1}$  may be ascribed to  $\text{C}\equiv\text{N}$  stretching vibrations of amines.<sup>26</sup> The peaks at  $1643\text{ cm}^{-1}$  and  $1525\text{ cm}^{-1}$  indicate the presence of C=O or C=C bonds in carboxylic acids or aromatic compounds, and the peak at  $1376\text{ cm}^{-1}$  corresponds to C–O stretching vibrations in alcohols or ethers. The peaks at  $943\text{ cm}^{-1}$ ,  $820\text{ cm}^{-1}$  and  $685\text{ cm}^{-1}$  may correspond to the C–X bond of alkyl halides and C–H bond stretching of aromatic compounds.<sup>27</sup> The FTIR spectrum of the synthesized NiO nanoparticles showed a peak at  $3519\text{ cm}^{-1}$  and diminished peaks on either side, indicating the presence of many O–H groups as in polyols, present in different environments. The other peaks at  $1637\text{ cm}^{-1}$ ,  $1368\text{ cm}^{-1}$  and  $1117\text{ cm}^{-1}$  showed the presence of secondary metabolites and proteins, which are mainly responsible for stabilizing the NiO NPs through complexation.<sup>12</sup>

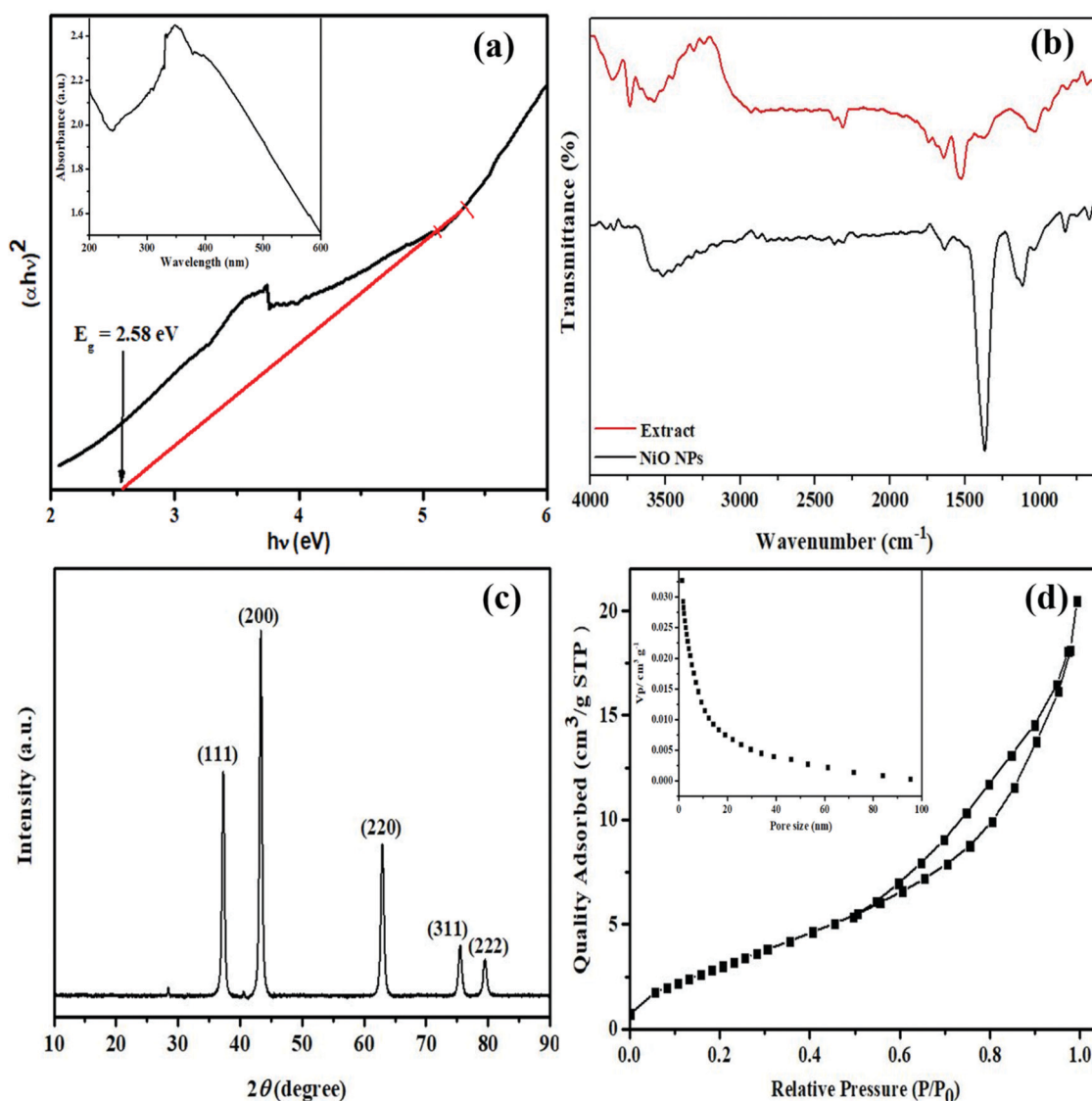


Fig. 1 (a) Tauc plot (inset UV-vis spectra); (b) FTIR spectra of the extract; (c) XRD pattern and (d) BET (inset: pore size distribution) of the NiO NPs.





The peaks at 671 and 831  $\text{cm}^{-1}$  are in the range of metal–oxygen stretching vibrations, indicating the presence of a Ni–O bond.<sup>2</sup>

The structural and crystallinity information of NiO NPs is displayed in Fig. 1c. The XRD pattern affirmed the formation of NiO nanoparticles with intense reflection peaks at  $2\theta = 37.3$ , 43.3, 62.9, 75.6 and 79.6 with indices (111), (200), (220), (311) and (222), respectively. The diffraction pattern obtained for the synthesized nanoparticles was in good agreement with JCPDS card number 47–1049, with a face-centred cubic structure of NiO NPs having average lattice parameter of 4.17710 Å.<sup>28</sup> The average crystallite size of the nanoparticles was found to be 27.7 nm as calculated using the classical Debye–Scherrer approximation. These results are in agreement with the TEM results. The large surface area of nanomaterials offers an incredible opportunity for assorted applications. The BET analysis of the as synthesized NiO NPs has been displayed in Fig. 1d. The specific surface area, average pore size and total pore volume of NiO NPs were evaluated to be 16.71  $\text{m}^2 \text{g}^{-1}$ , 1.2 nm and 0.32  $\text{cm}^3 \text{g}^{-1}$ , respectively, using the BJH method. This suggests that NiO NPs are mesoporous with moderately uniform pore size distribution.

The vibrational modes of the as-synthesized NiO NPs were also investigated using Raman spectroscopy (Fig. 2). In the NiO NPs, four scattering peaks were observed at 501, 735, 1080 and 1460  $\text{cm}^{-1}$ . These could be ascribed to the first-order longitudinal optical phonon mode of the Ni–O lattice vibrations, the second-order transverse, and the longitudinal optical phonon modes,<sup>29,30</sup> and the two-magnon mode of NiO.<sup>31</sup>

The surface morphological characteristics of the as-synthesized NiO NPs were examined by field emission scanning electron microscope (FESEM) and shown in Fig. 3(a and b). It has been observed that nanoparticles have a spherical shape with some level of agglomeration which might be ascribed to the high surface energy and surface tension of the NiO NPs.<sup>32</sup> Energy dispersive X-ray analysis (EDX) was used to confirm the elemental composition and purity of the NiO nanoparticles. The EDX precisely quantified the Ni and O contents, and

exhibited only Ni and O peaks without any other peak due to contaminants (Fig. 3b).

HRTEM investigations were employed to explore the morphology and structure of the NiO NPs. Fig. 4(a–c) displays the HRTEM images of NiO NPs and confirm the formation of agglomerated quasi spherical particles. The sharp diffraction spots in the selected area electron diffraction (SAED) pattern (Fig. 4d) suggest that the as-obtained nanoparticles are polycrystalline and indexed to (111), (200), (220), (311) and (222), respectively, and these observations are in good agreement with the XRD results.

The survey spectrum (Fig. 5a) displays the characteristic binding energy (eV) peaks corresponding to Ni, O and C in the nanoparticles. The obtained Ni 2p spectrum supports Ni 2p<sub>3/2</sub> and Ni 2p<sub>1/2</sub> peaks. Fig. 5b demonstrates that the characteristic peaks of Ni<sup>2+</sup> 2p<sub>3/2</sub>, and its satellite peaks were found at 854.1, 855.6, and 861.2 eV, respectively, whereas the Ni<sup>2+</sup> 2p<sub>1/2</sub> peak was found at 872.6 eV, indicating that NiO structures were formed.<sup>33</sup> The deconvoluted spectra of oxygen (O 1s) in Fig. 5c revealed a peak at 529.6 eV, which is related to the peak in Ni 2p (NiO). The other peak at 531.2 eV was attributed to the C=O group or shoulder peak of NiO. The peaks at 285.3, and 284.9 eV were assigned to the C–OH/C–O–Ni, and C–C/C=C, respectively, in the deconvoluted expanded spectra of C 1s (Fig. 5d).

## Biological applications

### Antibacterial activity

Currently, a number of traditional medicines having antibiotic potential are in use to control bacterial infections throughout the world. But, one of the major problems associated with the use of traditional antibiotic medicines is the development of antibiotic resistance in bacteria. The scientific community from around the world is working hard for developing alternative materials having strong antibiotic potential with no risk of antibiotic resistance to control the infectious bacterial diseases.<sup>34–36</sup> The recent advances in nanotechnology have great potential for providing new materials with significant antimicrobial properties through promising eco-friendly routes.<sup>37–39</sup>

In this study, the antibacterial activity of the as-synthesized NiO NPs using cell free extract of *Spirogyra* sp. was evaluated by determining the growth rate of selected bacterial strains: Gram-positive (*B. subtilis*) and Gram-negative (*E. coli*). The selected test organisms were cultured in LB medium supplemented with graded concentrations (0 to 15  $\text{mg L}^{-1}$ ) of NiO NPs and their growth rate was monitored regularly in terms of optical density at 600 nm. The obtained results revealed that the synthesized NiO NPs showed a dose-dependent response against both the selected bacterial strains (Fig. 6). Moreover, the cell free extract of *Spirogyra* sp. also exhibited an inhibitory effect on the growth of both the tested organisms in comparison to the control (growth medium without nanoparticles). The biosynthesized NiO NPs showed strong antibacterial activity by inhibiting the growth of both the bacterial strains within the first 2 h of the

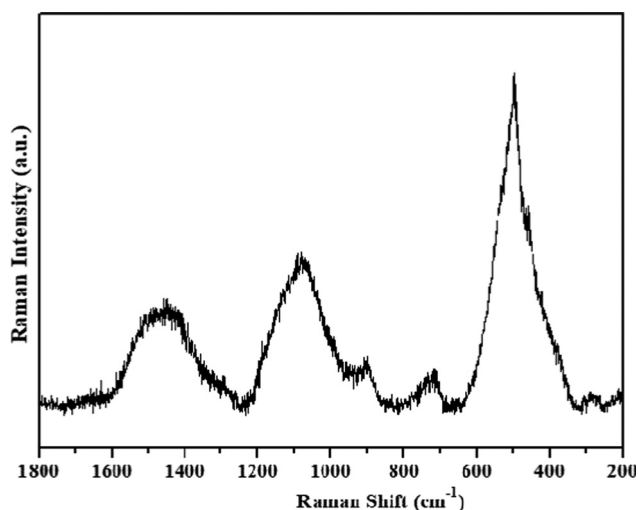


Fig. 2 Raman spectrum of NiO NPs.



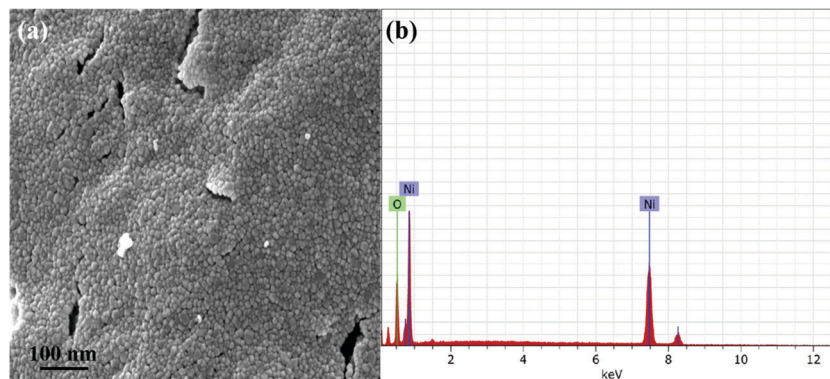


Fig. 3 (a) FESEM image; (b) EDX spectra of NiO nanoparticles.

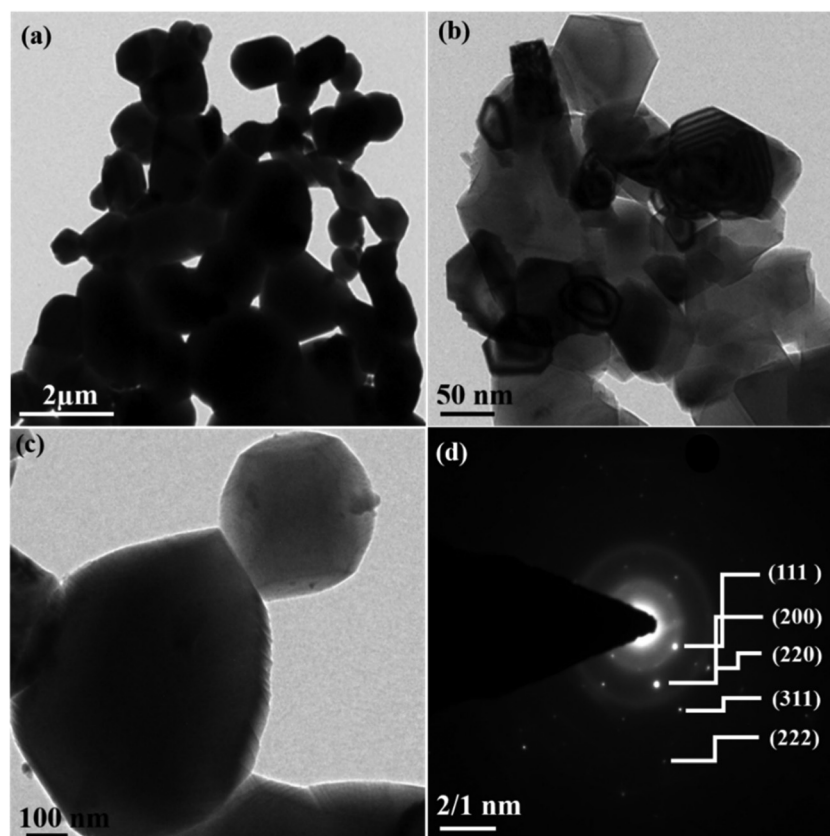


Fig. 4 HRTEM images (a–c) and (d) SAED pattern of NiO NPs.

experiment at 10 and 15 mg L<sup>-1</sup> concentrations. The MIC of the biosynthesized NiO NPs for bacterial growth was found to be 10 mg L<sup>-1</sup> for both the bacterial strains. The obtained results confirmed that the NiO NPs synthesized using cell free extract of *Spirogyra* sp. are bacteriostatic at lower concentration while bactericidal at higher concentration. The results also suggested that 10 mg L<sup>-1</sup> concentration of the as-synthesized NiO NPs was suitable to act as a viable bactericidal for preventing bacterial contamination. Overall, the biogenic NiO NPs synthesized in this study showed significant antibacterial potential, which is consistent with the previous reports.<sup>28,35,36,39,40</sup> The exact

mechanism for the antibacterial action of NiO NPs is still not well described. So, it may be hypothesized here that the nanoparticles having ~25–30 nm size easily infiltrate the bacterial cell wall and interact with the various cytoplasmic biomolecules of bacteria. The bio-compounds on the surface, and the charge and size of the nanoparticles are the key attributes that contribute to adsorption of NPs on bacterial cells and their smooth penetration inside the cell by disrupting cell wall integrity. The penetration of NPs inside the cell may cause oxidative stress by generating reactive oxygen species (ROS), which leads to cellular oxidative damage and NPs-based toxicity. The earlier studies have also



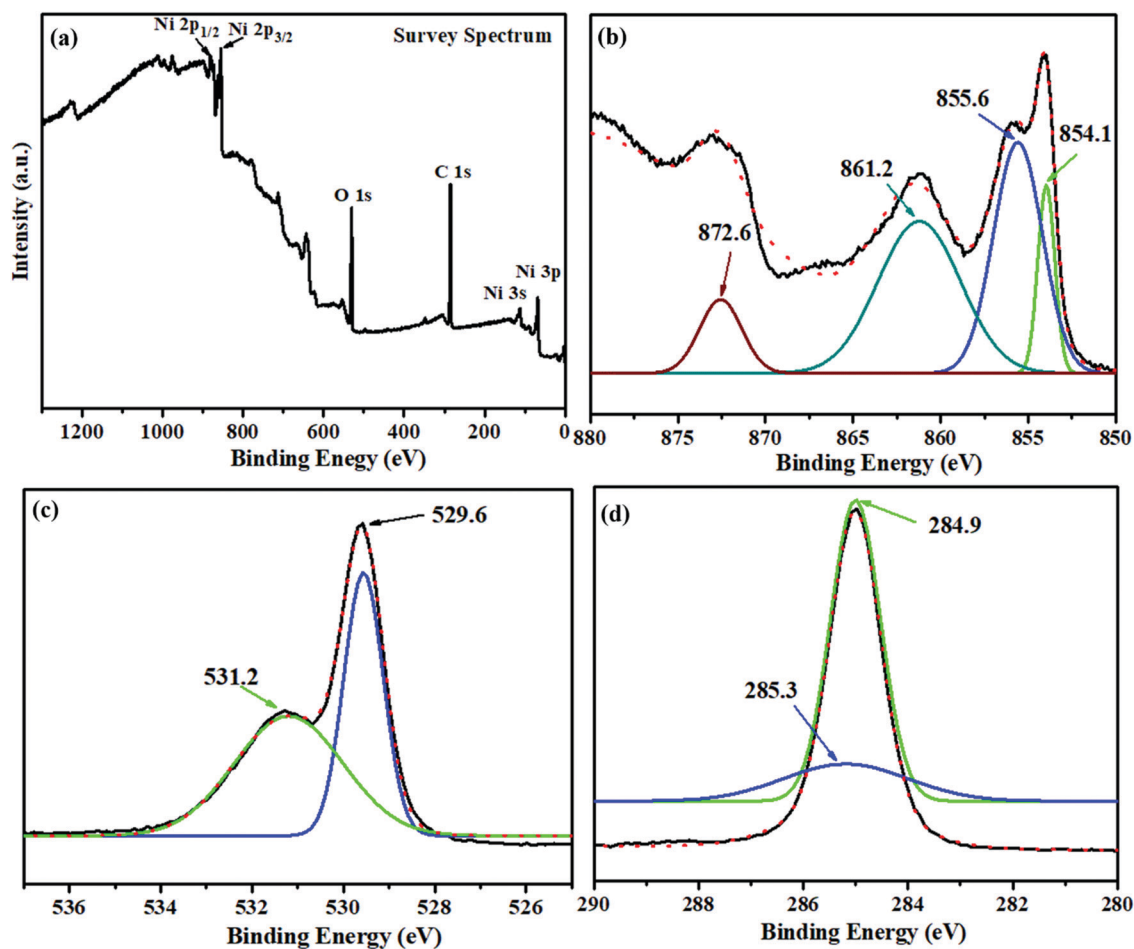


Fig. 5 XPS spectra of NiO NPs.

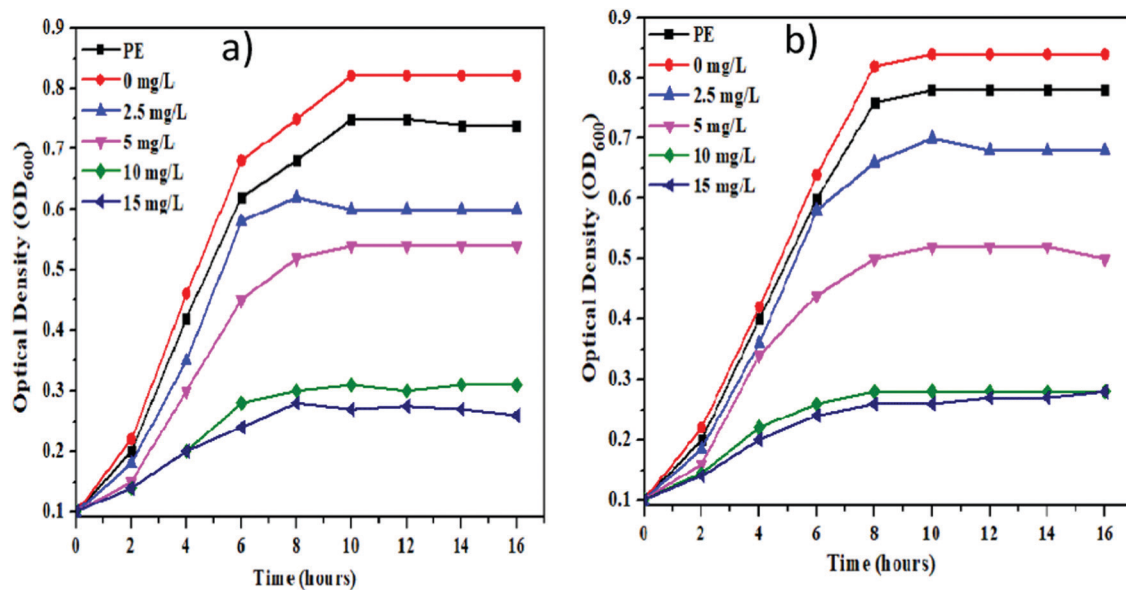


Fig. 6 Growth curves of selected bacterial strains, (a) *B. subtilis* and (b) *E. coli* at different concentrations of the synthesized NiO NPs.





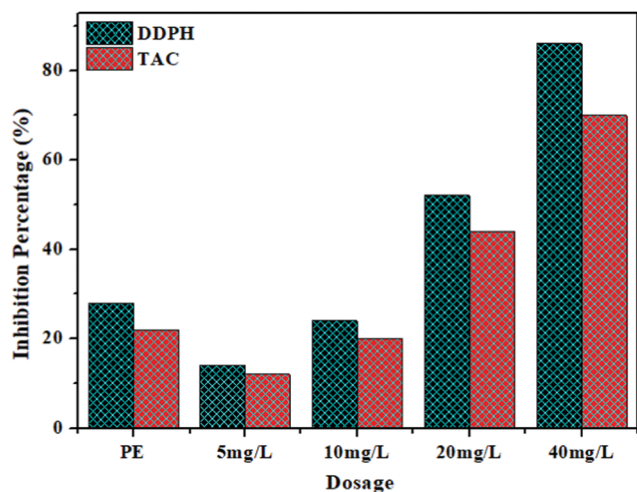


Fig. 7 Antioxidant activity of biogenic NiO NPs at different concentrations.

concluded that biogenic NPs can easily infiltrate the cell wall and cause cell death by oxidative damage.<sup>32,37</sup>

### Antioxidant activity

The biogenically synthesized NiO NPs were found to have strong DPPH radical scavenging ability in comparison to that of the algal extract. The obtained results indicate that all the tested samples have concentration-dependent antioxidant activity, *i.e.* from 28% to 86% across all the tested concentrations ranging from 5 mg L<sup>-1</sup> to 40 mg L<sup>-1</sup> (Fig. 7). Furthermore, the total antioxidant capacity of the biosynthesized NiO NPs supports their free radical scavenging potential. The maximum value for total antioxidant capacity (TAC) in terms of ascorbic acid per mg was found to be 70% for 40 mg L<sup>-1</sup> of NiO NPs. It is noteworthy that cell free extract of *Spirogyra* sp. also exhibited good free radical scavenging activity and total antioxidant capacity. These observations indicated that cell free extract of *Spirogyra* sp. is a rich source of natural antioxidants. Therefore, the algal biomolecules (flavonoids, phenolic acids, alkaloids, *etc.*) present on the surface of the nanoparticles were responsible for the high antioxidant activity of the synthesized NiO NPs. The results of antioxidant activity studies are in agreement with earlier reports on biogenic NiO NPs.<sup>20,38,39</sup>

### Effect on seed germination and seedling growth

Recently, NPs based bio-fertilizers have emerged as a better substitute with significant applications in agriculture fields to enhance nutrient uptake, break seed dormancy and reduce the use of hazardous agrochemicals. Therefore, NPs synthesized by a green route have better potential and are an eco-friendly alternative to agrochemicals used in agriculture fields. Presently, numerous metallic nanoparticles including TiO<sub>2</sub>, ZnO and Ag NPs *etc.* are in use for sustainable agriculture.<sup>40–42</sup> In the present study, the effect of the synthesized NiO NPs on seed germination and early seedling growth (Root and Shoot Length) of Mung Bean was examined on the 4th and 8th day of the experiment. The obtained results indicated that the synthesized NiO NPs at low concentration (5 mg L<sup>-1</sup>) showed a stimulatory effect on seed germination and early seedling growth of mung beans in comparison to the non-treated control. It is worth mentioning that the cell free extract of *Spirogyra* sp. also exhibited a stimulatory effect on all the studied growth parameters. Although at lower concentration of NPs, the seed germination was not inhibited, at higher concentrations, the germination was inhibited by 16, 45 and 80% at 10, 20 and 40 mg L<sup>-1</sup>, respectively. A significant increase (nearly 15%) in the root length of 4.1 and 9.2 cm was observed on 4th and 8th day, respectively at 5 mg L<sup>-1</sup> concentration of the synthesized NiO NPs in comparison to the non-treated control (Fig. 8b and c). A similar trend was observed in the case of shoot length in which a significant increase of 20% and 21.22% was observed on the 4th and 8th day, respectively at 5 mg L<sup>-1</sup> concentration of the synthesized NiO NPs in comparison to the non-treated control. However, higher concentrations (>10 mg L<sup>-1</sup>) of the synthesized NiO NPs caused a significant reduction in root and shoot length of mung beans. Results of this investigation corroborate with findings of previous studies that showed both inhibitory and stimulatory effects of NiO NPs on seed germination and seedling growth of various crops.<sup>39,43–47</sup>

### Conclusion

This study demonstrates an ecofriendly method for the synthesis of biogenic NiO NPs using cell free extract of green macroalgae *Spirogyra* sp. The physical characterization of the

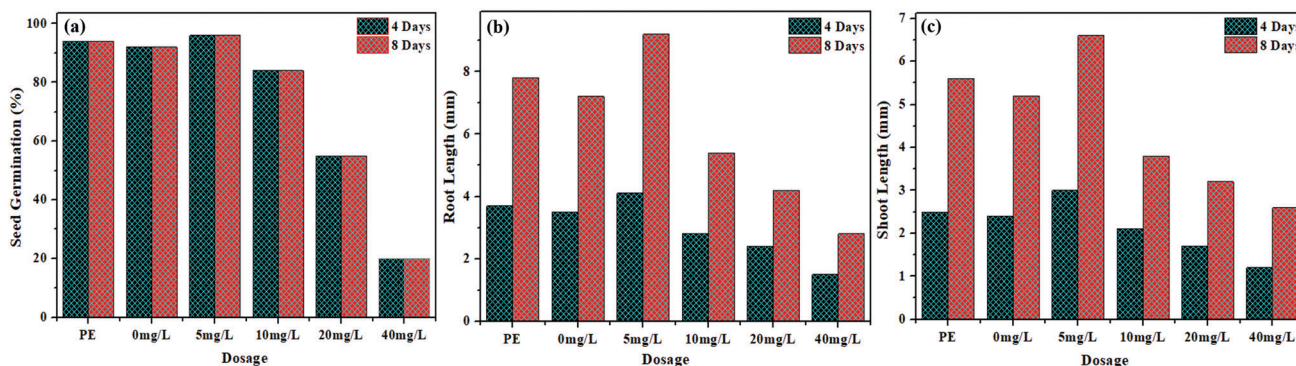


Fig. 8 Effect of the synthesized NiO NPs on (a) seed germination, (b) root length and (c) shoot length.





as-synthesized NPs by various sophisticated methods revealed the stable polycrystalline nature of the as-synthesized NiO NPs with assorted morphological properties, controlled size (27.7 nm) with large surface area and semiconducting nature ( $E_g = 2.85$  eV) along with the confirmation of bioactive functional groups on the surface. The biogenic NiO NPs exhibited various *in vitro* biological activities due to their small size and the presence of capping and stabilizing biomolecules on their surface. The synthesized NiO NPs have shown good antibacterial activity against Gram-positive (*Bacillus subtilis*) and Gram-negative (*Escherichia coli*) bacterial strains along with significant antioxidant activity. Moreover, the biogenically synthesized NiO NPs possess a stimulatory effect on seed germination and seedling growth of Mung Beans (*Vigna radiata*) at lower concentration ( $5 \text{ mg L}^{-1}$ ) which may be used as a substitute for synthetic agrochemicals for plants having seed dormancy and slow seed germination. Hence, it is concluded that the as-synthesized biogenic NiO NPs from cell-free extract of *Spirogyra* sp. with potential biological activities could be utilized as bactericides and green agrochemicals at industrial scale after carrying out detailed *in vivo* studies on their toxicity in animal models.

## Conflicts of interest

There are no conflicts to declare.

## References

- 1 B. Koul, A. K. Poonia and D. Yadav, Review microbe-mediated biosynthesis of nanoparticles: applications and future prospects, *Biomolecular*, 2021, **11**, 1–33.
- 2 A. A. Olajire and A. A. Mohammed, Green synthesis of nickel oxide nanoparticles and studies of their photocatalytic activity in degradation of polyethylene films, *Adv. Powder Technol.*, 2020, **31**, 211–218.
- 3 S. S. Sana, R. P. Singh, M. Sharma, A. K. Srivastava, G. Manchanda, A. R. Rai and Z. Zhang, Biogenesis and application of nickel nanoparticles: A review, *Curr. Pharm. Biotechnol.*, 2021, **22**, 808–822.
- 4 M. Ramesh and H. Nagaraja, Adsorption and photocatalytic properties of NiO nanoparticles synthesized via a thermal decomposition process, *Mater. Res.*, 2018, **33**, 601–610.
- 5 A. Singh, A. Singh, S. Singh, P. Tandon and R. R. Yadav, Synthesis, characterization and gas sensing capability of  $\text{Ni}_x\text{Cu}_{1-x}\text{Fe}_2\text{O}_4$  ( $0.0 \leq x \leq 0.8$ ) nanostructures prepared via Sol–Gel method, *J. Inorg. Organomet. Polym.*, 2016, **26**, 1392–1403.
- 6 A. M. Ayesha, M. Kashif, S. Arokiyaraj, M. G.-V. Sankaracharyulu, M. Jayachandran and U. Hasim, Bio-Synthesis of NiO and Ni nanoparticles and their characterization, *Dig. J. Nanomater. Biostructures*, 2014, **9**, 1007–1019.
- 7 Y. Singh, S. Kaushal and R. S. Sodhi, Biogenic synthesis of silver nanoparticles using cyanobacterium *Leptolyngbya* sp. WUC 59 cell-free extract and their effects on bacterial growth and seed germination, *Nanoscale Adv.*, 2020, **2**, 3972–3982.
- 8 N. Mayedwa, N. Mongwaketsi, S. Khamlich, K. Kaviyarasu, N. Matinise and M. Maaza, Green synthesis of nickel oxide, palladium and palladium oxide synthesized via *Aspalathus linearis* natural extracts: physical properties & mechanism of formation, *Appl. Surf. Sci.*, 2018, **446**, 266–272.
- 9 N. Matinise, X. G. Fuku, K. Kaviyarasu, N. Mayedwa and M. Maaza, ZnO nanoparticles via moringa oleifera green synthesis: physical properties & mechanism of formation, *Appl. Surf. Sci.*, 2017, **406**, 339–347.
- 10 Z. Sanaeimehr, I. Javadi and F. Namvar, Antiangiogenic and antiapoptotic effects of green-synthesized zinc oxide nanoparticles using sargassum muticum algae extraction, *Cancer Nanotechnol.*, 2018, **9**, 1–16.
- 11 Z. Salari, F. Danafar, S. Dabaghi and S. A. Ataei, Sustainable synthesis of silver nanoparticles using macroalgae *Spirogyra* and analysis of their activity, *J. Saudi Chem. Soc.*, 2016, **20**, 459–464.
- 12 R. Chaudhary, K. Nawaz, A. K. Khan, C. Hano, B. H. Abbasi and S. Anjum, An overview of the algae-mediated biosynthesis of nanoparticles and their biomedical applications, *Biomolecular*, 2020, **10**, 1–36.
- 13 P. Bhuyar, M. H.-A. Rahim, S. Sundararaju, R. Ramaraj, G. P. Maniam and N. Govindan, Synthesis of silver nanoparticles using marine macroalgae *Padina* sp. and its antibacterial activity towards pathogenic bacteria, *J. Basic Appl. Sci.*, 2020, **9**, 1–15.
- 14 G. Ghodake and D. S. Lee, Biological synthesis of gold nanoparticles using the aqueous extract of the brown algae *Laminaria japonica*, *J. Nanoelectron. Optoelectron.*, 2017, **6**, 268–271.
- 15 S. Sudhasree, A. Shakila Banu, P. Brindha and G. A. Kurian, Synthesis of nickel nanoparticles by chemical and green route and their comparison in respect to biological effect and toxicity, *Toxicol. Environ. Chem.*, 2014, **96**, 743–754.
- 16 M. I. Din, M. Tariq, Z. Hussain and R. Khalid, Single step green synthesis of nickel and nickel oxide nanoparticles from *Horedeum vulgare* for photocatalytic degradation of methylene blue dye, *Inorg. Nano-Met. Chem.*, 2020, **50**, 1–6.
- 17 C. J. Pandian, R. Palanivel and S. Dhananasekaran, Green synthesis of nickel nanoparticles using *Ocimum sanctum* and their application in dye and pollutant adsorption, *Chin. J. Chem. Eng.*, 2015, **23**, 1307–1315.
- 18 M. I. Din, A. G. Nabi, A. Rani, A. Aihetasham and M. Mukhtar, Single step green synthesis of stable nickel and nickel oxide nanoparticles from *Calotropis gigantea*: Catalytic and antimicrobial potentials, *Environ. Nanotechnol., Monit. Manage.*, 2018, **9**, 29–36.
- 19 H. Chen, J. Wang and D. Huang, *et al.*, Plant-mediated synthesis of size-controllable Ni nanoparticles with alfalfa extract, *Mater. Lett.*, 2014, **122**, 166–169.
- 20 M. I. Khan, N. Fatima, M. Shakil, M. B. Tahir, K. N. Riaz, M. Rafique, T. Iqbal and K. Mahmood, Investigation of *in vitro* antibacterial and seed germination properties of green, *Phys. B*, 2021, **601**, 412563.



- 21 S. Srihasam, K. Thyagarajan, M. Korivi, V. R. Lebaka and S. P. Mallem, Phytogetic generation of NiO nanoparticles using Stevia leaf extract and evaluation of their in-vitro antioxidant and antimicrobial properties, *Biomolecular*, 2020, **10**, 89.
- 22 R. Junthip, D. Amornlerdpison and T. Chimsook, Phytochemical screening antioxidant activity and total phenolic content of spirogyra spp., *Adv. Mater. Res.*, 2013, **699**, 693–697.
- 23 P. Champa, N. Whangchai, S. Jaturonglumlert, N. Nakao and K. Whangchai, Internat. Determination of phytochemical compound from spirogyra sp. using ultrasonic assisted extraction, *J. GEOMATE*, 2016, **11**, 2391–2396.
- 24 A. Najlaa, S. Al-Radadi, T. Hussain, S. Faisal, S. Ali and R. Shah, Novel biosynthesis, characterization and biocatalytic potential of green algae (*Spirogyra hyaline*) mediated silver nanomaterials, *Saudi J. Biol. Sci.*, 2022, **29**, 411–419.
- 25 V. Helan, J. Prince, N. A. A-Dhabi and M. Jayachandran, Neem leaves mediated preparation NiO nanoparticles and its magnetization, coercivity and antibacterial analysis, *Results Phys.*, 2016, **6**, 712–718.
- 26 P. Prieto, M. Pineda and M. Aguliar, Spectrophotometric quantitation of antioxidant capacity through the formation of phosphomolybdenum complex: specific application to the determination of vitamin E, *Biochemistry*, 1999, **269**, 337–341.
- 27 H. J.-S. Hawezy, K. H. Sdiq, V. A. Qadr, S. S. Anwer and S. J. Salih, Biosynthesis of magnetite-nanoparticles using microalgae (*Spirulina* sp. and *Spirogyra* sp.), *Indian J. Public Health Res. Dev.*, 2020, **11**, 1–7.
- 28 A. A. Ezhilarasi, J. J. Vijaya, K. Kaviyarasu, L. J. Kennedy, R. J. Ramalingam and H. A. Al-Lohedan, Green synthesis of NiO nanoparticles using *Aegle marmelos* leaf extract for the evaluation of in-vitro cytotoxicity, antibacterial and photocatalytic properties, *J. Photochem. Photobiol., B*, 2018, **180**, 39–50.
- 29 H. Wang, H. Yi and X. Wang, Asymmetric supercapacitors based on nano-architected nickel oxide/graphene foam and hierarchical porous nitrogen-doped carbon nanotubes with ultrahigh-rate performance, *J. Mater. Chem. A*, 2014, **2**, 3223–3230.
- 30 X. Rong, F. Qui, J. Qin, H. Zhao, J. Yan and D. Yang, A facile hydrothermal synthesis, adsorption kinetics and isotherms to Congo Red azo-dye from aqueous solution of NiO/graphene nanosheets adsorbent, *J. Ind. Eng. Chem.*, 2015, **26**, 354–363.
- 31 Z. Qiu, Y. Ma and T. Edvinsson, In operando Raman investigation of Fe doping influence on catalytic NiO intermediates for enhanced overall water splitting, *Nano Energy*, 2019, **66**, 104118.
- 32 H. G. Gebretinasae, M. G. Tsegay and Z. Y. Nuru, Biosynthesis of nickel oxide (NiO) nanoparticles from cactus plant extract, *Mater. Today: Proc.*, 2021, **36**, 566–570.
- 33 B. A. Abbasi, J. Iqbal, T. Mahmood, A. T. Khalil, B. Ali, S. Kanwal and R. Ahmad, Role of dietary phytochemicals in modulation of miRNA expression: natural swords combat breast cancer, *Asian Pac. J. Trop. Med.*, 2018, **11**, 501–509.
- 34 N. Woodford and D. M. Livermore, Infections caused by Gram-positive bacteria: a review of the global challenge, *J. Infect.*, 2009, **59**, 4–16.
- 35 B. A. Abbasi, J. Iqbal, T. Mahmood, R. Ahmad, S. Kanwal and S. Afridi, Plant-mediated synthesis of nickel oxide nanoparticles (NiO) via *Geranium wallichianum*: characterization and different biological applications, *Mater. Res. Express*, 2019, **6**, 850–857.
- 36 L. Rizzello, R. Cingolani and P. P. Pompa, Nanotechnology tools for antibacterial materials, *Nanomedicine*, 2013, **8**, 807–821.
- 37 M. U. Munir, A. Ahmed, M. Usman and S. Salman, Recent advances in nanotechnology-aided materials in combating microbial resistance and functioning as antibiotics substitutes, *Int. J. Nanomed.*, 2020, **15**, 7329–7358.
- 38 B. Y. Hussein and A. M. Mohammed, Biosynthesis and characterization of nickel oxide nanoparticles by using aqueous grape extract and evaluation of their biological applications, *Results Chem.*, 2021, **3**, 100142.
- 39 A. T. Khalil, M. Ovais, I. Ullah, M. Ali, Z. K. Shinwari, D. Hassan and M. Maaza, *Sageretia thea* (Osbeck.) modulated biosynthesis of NiO nanoparticles and their in vitro pharmacognostic, antioxidant and cytotoxic potential, *Nanomed. Biotechnol.*, 2018, **46**, 838–852.
- 40 S. Uddin, L. B. Safdar, S. Anwar, J. Iqbal, S. Laila, B. A. Abbasi, M. S. Saif, M. Ali, A. Rehman and A. Basit, Green synthesis of nickel oxide nanoparticles from *Berberis balochistanica* stem for investigating bioactivities, *Molecules*, 2021, **26**, 1548.
- 41 N. Younes, H. S. Hassan, M. F. Elkady, A. Hamed and M. F. Dawood, Impact of synthesized metal oxide nanomaterials on seedlings production of three Solanaceae crops, *Heliyon*, 2020, **6**, 3188.
- 42 L. A. Paramo, A. A. Feregrino-Pérez, R. Guevara, S. Mendoza and K. Esquivel, Nanoparticles in agroindustry: applications, toxicity, challenges, and trends, *Nanomaterials*, 2020, **10**, 1654.
- 43 D. Mittal, G. Kaur, P. Singh, K. Yadav and S. A. Ali, Nanoparticle-based sustainable agriculture and food science: recent advances and future outlook, *Front. Nanotechnol.*, 2020, **2**, 579954.
- 44 M. Faisal, Q. Saquib, A. A. Alatar, A. A. Al-Khedhairi, A. K. Hegazy and J. Musarrat, Phytotoxic hazards of NiO-nanoparticles in tomato: A study on mechanism of cell death, *J. Hazard. Mater.*, 2013, **250**, 318–332.
- 45 M. A. Korotkova, S. V. Lebedev and F. G.-K. Sizova, Biological effects in wheat (*Triticum vulgare* L.) under the influence of metal nanoparticles (Fe, Cu, Ni) and their oxides (Fe<sub>3</sub>O<sub>4</sub>, CuO, NiO), *Agrobiology*, 2017, **52**, 172–182.
- 46 A. M. Saleh, Y. M. Hassan, S. Selim and H. AbdElgawad, NiO-nanoparticles induce reduced phytotoxic hazards in wheat (*Triticum aestivum* L.) grown under future climate CO<sub>2</sub>, *Chemosphere*, 2019, **220**, 1047–1057.
- 47 S. Chaudhary, Y. Kaur, B. Jayee, G. R. Chaudhary and A. Umar, NiO nanodisks: highly efficient visible light driven photocatalyst, potential scaffold for seed germination of *Vigna Radiata* and antibacterial properties, *J. Cleaner Product.*, 2018, **190**, 563–576.

